

COMPARATIVE ANALYSIS OF DIFFERENT TYPES OF ANTENNA STRUCTURES BY USING DIFFERENT FEEDING TECHNIQUES

Dr. Swati Sharma¹, Yazdan Khan²

¹Associate Professor, ²Ph.D. Scholar, Jodhpur National University, Jodhpur

Abstract: Helical antennas are basically broadband antennas which provide high gain, with larger real input impedance. The most important factor is that they produce circularly polarized wave at the antenna output terminal. A modified form of the helix, the spherical helix, has been shown to generate similar polarization and gain characteristics over a narrow bandwidth but a much larger beamwidth. This paper gives the comparison of different spherical helical antenna structures by using softwares like 4NEC2, MININEC Pro and CST studio also with the help of MATLAB. The results which are produced experimentally with the help of prototype and also by simulating the different parametric attributes provide such a platform for analyzing and comparing the different parameters for different types of helical antennas two specific results with some desirable radiation properties.

Keywords: Helical Antenna; bifilar Helical Antenna; QHA; Feeding techniques.

I. INTRODUCTION

The study of the design of different antenna structures and their characteristic gives the novel ideas to find the solution for many parametric design consideration approaches to overcome the many of the problems associated with the antenna design as there are variety of antenna parameters which depend upon the types of antennas antenna selection approaches, their feeder mechanism and the selection of the frequency of operation. Here we have examined and studied the different helical antenna structures and their properties related to these specific types of structures which is basically categorized in four types of filler topologies like monofilar, bifilar, quadifilar and multifilar with Their basic design considerations with respect to feeding techniques.

By studied in detail both numerically and experimentally with the help of available standard results also with help of different softwares like mat lab and mininec and online available tools and making tables of their different parameters of the proposed different multifilar hemispherical helices. Different characteristics and parameters like gain, Directivity, E- and H-plane radiation patterns, axial ratio and input impedance are calculated and simulated. This orientation of research paper is targeted as comparative analysis of different antenna design. It is shown that the bifilar hemispherical helix provides a flat gain curve over the measured bandwidth (~14%) and generally elliptical polarization with near circular polarization in limited case.

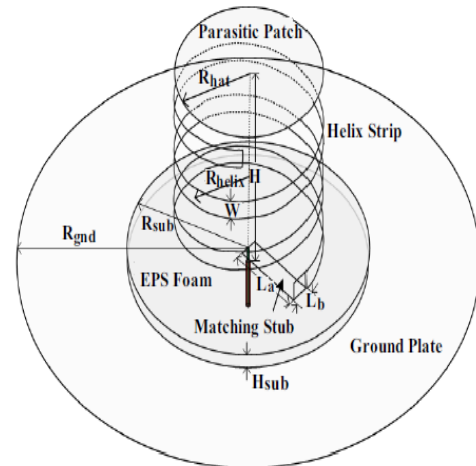
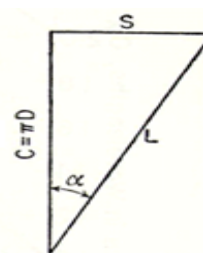


Fig 1.1 : Basic Design of helical antenna.

Figure 1.2 shows some relevant relations among the parameters of the helix are summarized below. These include the proportional relationship of the circumference (C) and diameter (D), since the helix has a circular cross section, and the number of turns (N) in terms of the height (h) and turn spacing (S), since each turn corresponds to a given distance on the helical axis and the height of the helix is the total distance along the axis. The relationships for the length of one turn (L) and the pitch angle (α) may be found using simple right triangle trigonometry.



$$C = \pi D \quad (\text{Eq. 1.1})$$

$$L = \sqrt{(S^2 + C^2)} \quad (\text{Eq. 1.2})$$

$$\alpha = \arctan(S/C) \quad (\text{Eq. 1.3})$$

$$H = NS \quad (\text{Eq. 1.4})$$

Fig.1.2: helix geometry and basic equations

The Quadrifilar & The Bifilar Helical Antenna

One particular form of the quadrifilar version is the so-called resonant quadrifilar helix antenna, or volute antenna, which produces a broad circularly polarized endfire beam. This antenna involves four half-wavelength windings which are fed at the open end and are shorted to the ground plane, as shown in Figure 1.3. These windings are in the range of quarter- to full-turn helices. A 90° phase shifter is used to feed the orthogonal pairs of helices in quadrature. An example pattern is shown in Figure 3.4. The volute antenna is not a broadband device, as it produces a small bandwidth of only several percent. This antenna finds an important

application in the Global Positioning System (GPS), where the small size and circular polarization are critical features. A bifilar-version of the Kraus/helix has been reported by Holtum. This antenna is constructed of two coaxial helical wires on the diameters of the supporting cylinder. Each conductor is fed against a ground screen with the exciting currents in phase opposition. This differs from the backfire bifilar helical antenna in which the conductors are fed at one end, one against the other, without the presence of a ground screen. A backfire monofilar helix is shown to have substantially the same radiation characteristics "as the backfire bifilar helix. The monofilar helix, however, is more difficult to feed in" the backfire mode. The elements of the bifilar helix are fed in antiphase and produce a bifurcated beam, an example of which is depicted in Figure 3.5. Elements with appropriate phase differences, desirable patterns with very pure circular polarization may be obtained. In the case of the bifilar helix, the two elements are fed in antiphase, while the quadrifilar helix has adjacent elements fed in phase quadrature.

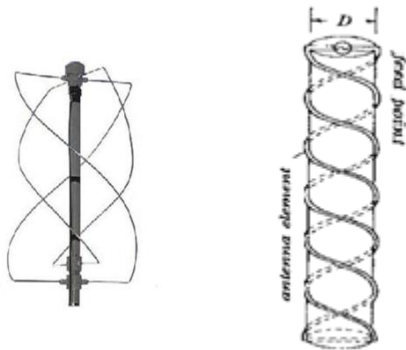


Fig 1.3: QHA (left) & BHA(right)

The Spherical helical antenna

The spherical helical antenna was first investigated by Cardoso and is shown in Figure 1.4. The spherical helix is a variation of the conventional helix that holds the spacing between turns (S) constant and varies the diameter (D) and pitch angle (α). The constant S condition implies that the spherical helix may be completely determined by the number of turns (N) and the radius of the sphere (r), be it an actual or fictitious sphere, since each turn must traverse the same distance along the axis.

$$r = a \text{ (Eq.1.5)}$$

$$\theta = \cos^{-1} \left(\frac{\phi}{N\pi} - 1 \right) \text{ (Eq.1.6)}$$

$$0 \leq \phi \leq 2\pi N \text{ (Eq.1.7)}$$

$$x = r \sin\theta \cos\phi \text{ (Eq.1.8)}$$

$$y = r \sin\theta \sin\phi \text{ (Eq. 1.9)}$$

$$z = r \cos\theta \text{ (Eq.1.10)}$$

The geometry of the spherical helix is well known and may be summarized in equations (1.5) through (1.7) using spherical coordinates (r, θ , ϕ). It is, first of all, noteworthy that each turn sweeps out 2π radians in the ϕ coordinate, yielding a total of $2\pi N$ radians for the entire spherical helix of N turns. Then, as ϕ varies from 0 to $2\pi N$. One advantage of the spherical helix over conventional cylindrical helices is the small electrical size. The axial length of the spherical helix is the same as the diameter, and thus the antenna is electrically very compact. For a spherical helix with a circumference of 1λ , the diameter is 0.3λ . The diameter, which is the primary

physical dimension of the antenna, is then rather small electrically in the axial mode regime.

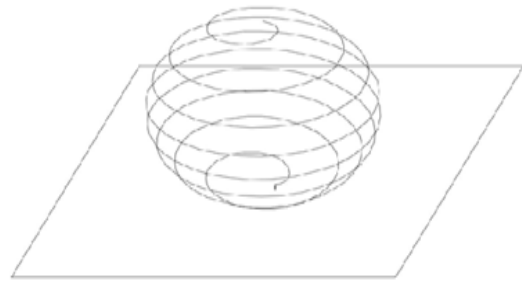


Fig 1.4 : spherical helical antenna.

Helix Radiation Modes

The helix has two operating regimes: the normal mode and the axial mode. The normal mode dominates when the wavelength of operation is larger than the diameter of the helix, whereas the axial mode dominates when the wavelength is smaller than the diameter. Of interest is the axial mode in which radiation is most intense along the axis of the helix and which produces a moderate gain and circular polarization for certain designs. It has been found that helices of several turns have acceptable characteristics when the electrical size (circumference) is between $\frac{3}{4}\lambda$ and 4λ , yielding a bandwidth of 56%. Figure 1.5 shows pattern plots for an axial mode and a normal mode helix obtained using the simulator program.

Normal Mode Analysis

Although analytical models of all but very simple antennas are difficult, if not impossible, to produce, the normal mode helix may be modeled as a small loop and small dipole, as shown in Figure 1.5. This, then, requires that the normal mode helix be small with respect to the wavelength of operation in terms of length and diameter. That is, $L \ll \lambda$ and $D \ll \lambda$. This analysis is independent of the number of turns and may proceed by examining a single turn. The resulting far-field pattern for the normal mode helix is the vector sum of the patterns resulting from the loop and the dipole individually. These are shown below with S being the spacing between turns (related to dipole length) and $D^2 \pi/4$ is the cross sectional area of the helix (related to the area of the loop).

$$E_D = j\omega\mu I S \frac{e^{j\beta r}}{4\pi r} \sin\theta \hat{\theta} \text{ (Eq.1.11)}$$

$$E_L = \eta\beta^2 \frac{\pi}{4} D^2 I \frac{e^{j\beta r}}{4\pi r} \sin\theta \hat{\phi} \text{ (Eq.1.12)}$$

$$F(\theta) = \sin\theta \text{ (Eq.1.13)}$$

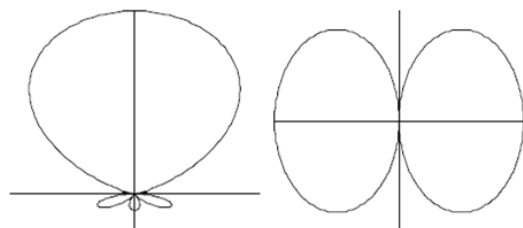


Fig 1.5 An axial mode & normal mode pattern

It is noted from equations (1.11) and (1.13) that these two components are 90° out of phase, and therefore can produce

circular polarization when equal in magnitude. The ratio of their magnitudes reduces to:

$$\frac{|E_{\theta}|}{|E_{\phi}|} = \frac{2S\lambda}{\pi^2 D^2} \text{ (Eq. 1.14)}$$

Setting (1.14) equal to 1 produces yields the condition for circular polarization. Using some of the geometrical relationships for the helix (equations (1.1) to (1.4)), the resulting condition reduces to the circular polarization condition in (1.15).

$$\alpha_{CP} = \sin^{-1} \left(\frac{-1 + \sqrt{1 + (L/\lambda)^2}}{L/\lambda} \right) \text{ (Eq. 1.15)}$$

Axial Mode Analysis

The axial mode helix can be approximated by modeling each turn as a simpler element in an array. Array theory may then be invoked and the radiation pattern found as the product of an N-element array (N-turn helix) pattern and the simplified element pattern. Since the helix performs best for axial mode with normalized circumferences between $\frac{3}{4} \lambda$ and $\frac{4}{3} \lambda$, each turn has a length of approximately one wavelength. Since the helix is essentially a traveling-wave antenna, and assuming the current is nearly constant along the wire, then the currents on opposite sides of the turn are about 180° out of phase. This means that these currents are nearly equivalent in direction, resulting in constructive interference of the radiation along the axis of the helix. This behavior is similar to the one-wavelength loop, and is easily seen when the pitch angle of the helix goes to zero, causing the antenna to degenerate into a loop. The element pattern of the array, then, is approximately $\cos \theta$, which is the pattern of the one-wavelength circular loop. Invoking array theory, the array factor, $AR(\theta)$, for an equally spaced N element (N-turn) linear array (helix) is expressed as:

$$F(\theta) = \frac{\sin(N\psi/2)}{N\sin(\psi/2)} \text{ (Eq. 1.16)}$$

where:

$$\psi = \beta S \cos\theta + \alpha_h \text{ (Eq. 1.17)}$$

with S being the element spacing, β the wave number, and α_h the inter-element phaseshift. The total pattern is then obtained as:

$$F(\theta) = K \cos\theta \frac{\sin(N\psi/2)}{N\sin(\psi/2)} \text{ (Eq. 1.18)}$$

where K is a normalization constant. It has been determined that the inter-element phaseshift, α_h is that of a Hansen-Woodyard array and is given as:

$$\alpha_h = - \left(\beta S + 2\pi + \frac{\pi}{N} \right) \text{ (Eq. 1.19)}$$

The normalization factor, K, can be found simply using the determined beam maximum along the axis of the helix (array), or $\theta = 0^\circ$. Then:

$$\psi = \beta S + \alpha_h = -2\pi - \frac{\pi}{N} \text{ (Eq. 1.20)}$$

$$F(0) = 1 = K \frac{\sin(-N\pi - \pi/2)}{N\sin(-\pi - \pi/2N)} \text{ (Eq. 1.21)}$$

Through the use of trigonometric identities:

$$K = (-1)^{N+1} N \sin(\pi/2N) \text{ (Eq. 1.22)}$$

The total pattern is then:

$$F(\theta) = (-1)^{N+1} \sin \left(\frac{\pi}{2N} \right) \cos\theta \frac{\sin \left(\frac{N\psi}{2} \right)}{\sin \left(\frac{\psi}{2} \right)} \text{ (Eq. 1.23)}$$

This result (Eq. 1.23) is an approximate analytical pattern for the helix based on array theory and is plotted in Figure 1.5.

The inclusion of an infinite ground plane is also possible by including the image of the helix (array) below the ground plane. Some empirical models for helix performance were produced by Kraus and then later, more intensively, by King and Wong. An empirical formula developed by King and Wong for the peak gain (G) is given in (1.24), where λ_p is the wavelength at peak gain.

$$G = 8.3 \left(\frac{\pi D}{\lambda_p} \right)^{\sqrt{N+2}-1} \left(\frac{NS}{\lambda_p} \right)^{0.8} \left(\frac{\tan 12.5^\circ}{\tan \alpha} \right)^{\sqrt{N}/2} \text{ (Eq. 1.24)}$$

Kraus has shown that the axial ratio is approximately given by (1.25) for an N-turn helix operating in the axial mode. This implies that the axial ratio approaches unity for a helix with a large number of turns.

$$AR = \frac{2N+1}{2N} \text{ (Eq. 1.25)}$$

It is noteworthy that this is specific to the helix. In general, the axial ratio is defined by (4.2.16). Left-hand circular polarization is represented by a '+' sign and right-hand circular polarization is represented by a '-' sign. A completely general method for calculating the axial ratio, given the magnitude and phase of the orthogonal components of the field, is available as well.

$$AR = \pm \frac{E_{majoraxis}}{E_{minoraxis}} \text{ (Eq. 1.26)}$$

An approximate formula for the input resistance of the helix is given by (1.27).

$$R_A = 140 \frac{c}{\lambda} \Omega \text{ (Eq. 1.27)}$$

The axial ratio and voltage standing wave ratio (VSWR) obtained from softwares for this antenna may also be compared to measured results. (In all cases in this investigation, the VSWR is in the form of a linear ratio rather than in decibels.) For both parameters, the simulated results follow the same general trends as those measured by Kraus. The greatest deviation occurs in the VSWR, where the simulated results yield slightly higher values over the middle to latter portion of the normalized circumference range, and very much higher values over the early portion of the range.

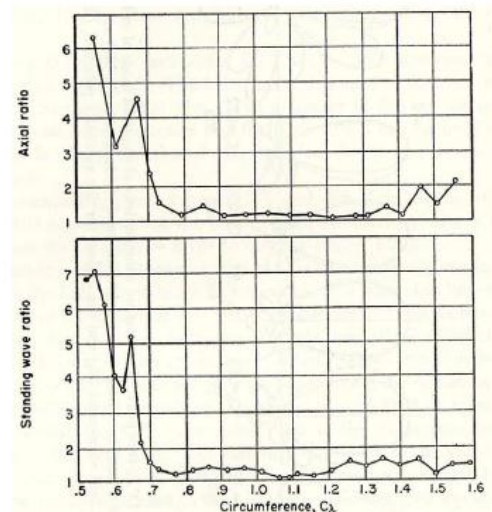


Fig 1.6: The measured values for axial ratio and VSWR for the 6 turn helix over a range of normalized circumferences

Feeding Methods

A feeding method is proposed for small helical antennas with diameters of about 1/80 to 1/20 wavelength. The present feeding method consists of excitation of a helix with a total length of about 1/4 wavelength and with its lower edge grounded by an open-ended center conductor oriented coaxially to the helix. In this paper, it is shown that matching with a 50-Ω feed system can be accomplished even when the helical diameter is varied in the same feeding method. The gain and the bandwidth characteristics of the ground plane versus diameter are discussed. As an example, a gain of -7.2 dB_d (with respect to the dipole antenna) on the ground plane is obtained when the helical diameter is 1/46 wavelength and the height is 1/56 wavelength. Like the monopole antenna, the main radiation pattern is omnidirectional vertical polarization in the horizontal plane and figure-eight in the vertical plane. When this antenna is installed on a transmitter case, the gain is about -4 dB_d. When installed on the transmitter case, the antenna radiates the orthogonal polarization component. The null of the main radiation pattern in the zenith direction can be compensated by this polarization. The radiation characteristics of the antenna are numerically calculated by the method of moments and are verified experimentally. The hemispherical helix may be fed in a number of ways. These include bottom fed (Figure 1.8), top-fed (Figure 1.9) and side-fed (Figure 1.10) configurations.

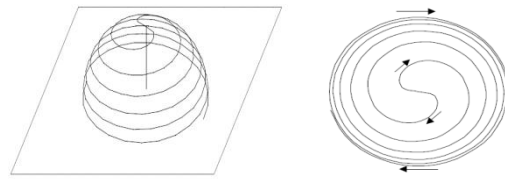


Fig 1.8 top fed bifilar hemispherical helix

The bifilar top-fed hemispherical helix involves a standard hemispherical helix with an identical helix rotated 180° about the axis, as shown in Figure 1.8. This variation of the hemispherical helix operates entirely in the axial-null mode due to the symmetry about the helical axis. Any current increment on one arm of the helix is matched by an equivalent current increment on the opposite arm. This yields a very large bandwidth for axial-null mode operation. If the bifurcated pattern of the axial-null mode is desirable, then there is a large frequency range available with this antenna for finding other advantageous radiation characteristics such as circular polarization or low VSWR at the feed point.

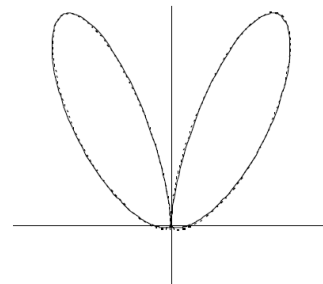


Fig 1.9 : The simulated radiation pattern bifilar hemispherical helix .

Since a very high VSWR at the feed point of the antenna is detrimental to the amount of radiation emitted, it is appropriate to concentrate on frequency ranges with a low VSWR. For the antenna under investigation, the range of interest corresponds to a normalized circumference range of about 2.5 λ to 3.1 λ, as can be seen in Figure 1.10. It was found that, in this range, the polarization is elliptical in general and circular in particular over limited beamwidths at some frequencies. Also of interest were those frequencies which produced circular polarization, which were limited to the range of approximately 2.7 λ to 3.1 λ. A plot of the axial ratio and phase difference between the θ and φ components of the electric field for the antenna in the H-plane is shown at one frequency in Figure 1.11.

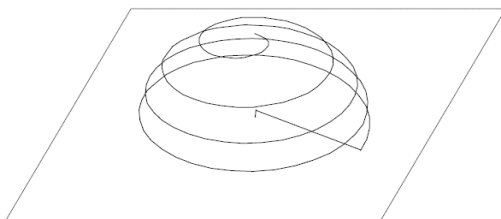


Fig 1.8 : bottom fed helix

Top-fed and bottom-fed hemispheres involve a wire from the feed point (at the origin) directly either upward to the apex (top) of the hemisphere or across to the termination of the helix near the ground plane (base). A side-fed hemisphere involves translation of the helix such that the termination of the wire is at the feed point.

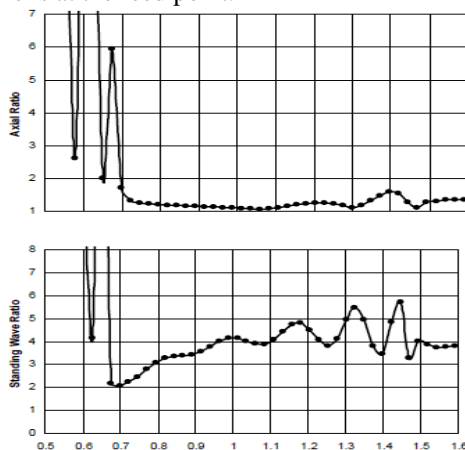


Fig 1.7: The measured values for axial ratio and VSWR for the 6 turn helix over a range of normalized circumferences

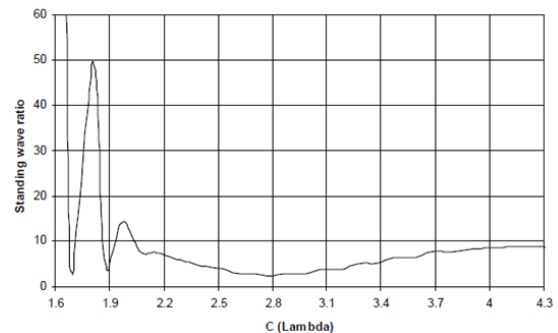


Fig 1.10: The simulated radiation pattern bifilar hemispherical helix .

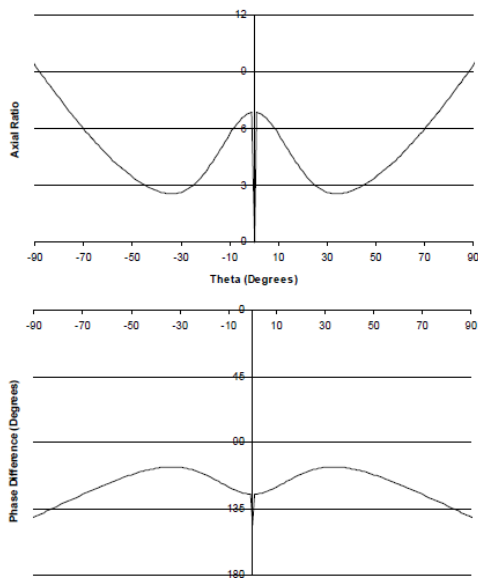


Fig 1.11 : The axial ratio (top) and phase difference (bottom) in the H plane for the bifilar hemispherical helix at a normalized circumference of 2.90λ

The Side-fed Quadrifilar Hemispherical Helix

The side-fed quadrifilar hemispherical helix is a variation that involves two bifilar hemispheres at 90° angles at the apex of the hemisphere. Figure 1.12 shows an example of this antenna. Using a side-feed on one arm, it is expected that the operation of this antenna will differ vastly from the top-fed bifilar hemisphere, since there will not be equal currents on each arm. Since the hemispherical helix is a traveling-wave antenna, it is likely that the current at the apex of the hemisphere will be low with respect to the feed point. The remaining current will likely be distributed among the other three arms or in reflection. It would appear, based on a brief evaluation, that this antenna will act largely like the standard hemispherical helix. It is hoped that the additional arms will improve the symmetry of the radiation patterns and possibly improve the polarization. The quadrifilar hemispherical helix was simulated over a normalized circumference range of 0.5λ to 2.3λ in increments of 0.1λ . As in

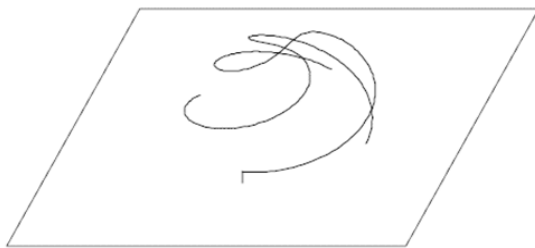


Fig 1.12 : The side fed quadrifilar hemispherical helix

The simulations of the bifilar antenna, 28 gauge conductor was used. Unlike with the bifilar hemispherical helix, the quadrifilar has no significant bandwidth with a reasonable VSWR, as shown in Figure 1.13. However, several resonances are present in which the VSWR falls below 2. Since method of moments codes are not always reliable for VSWR readings, it is possible that measurement may yield some more acceptable values. It was found that this antenna

produced largely linear polarization and a symmetrical axial beam over a reasonable bandwidth.

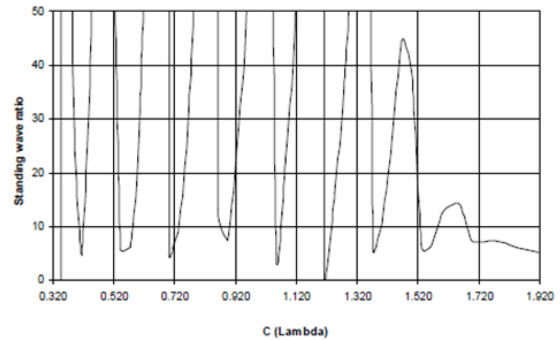


Fig 1.13: The simulated quadrifilar hemispherical helix. An example pattern is shown in Figure 1.14 that the simulated pattern in E- plane for the quadrifilar hemispherical helix at a normalized circumference of 0.80λ which has θ component (dashed) and ϕ component (solid) of the field.

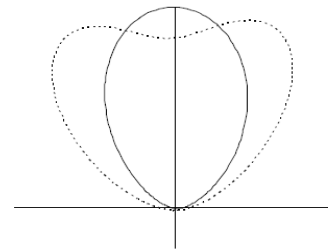


Fig 1.14 : The simulated pattern in E- plane for the quadrifilar hemispherical helix.

The axial ratio and phase difference for that pattern in Figure 5.12. It is noteworthy that the E- and H-planes have been defined in terms of the geometry of (Eq1.5) through (Eq1.7). The H-plane is the plane of $\phi = 2\pi n$, while the E-plane is $\phi = 2\pi n + \pi/2$. The measurements of the prototypes, discussed later, were made with this definition in mind.

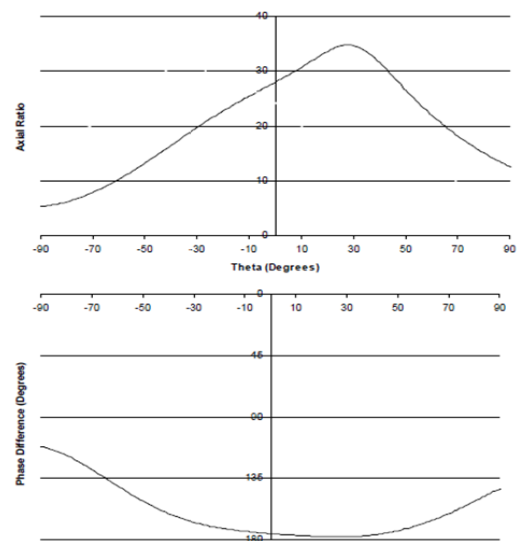


Fig 5.12 : The axial ratio (top) and phase difference (bottom) in the E – plane for the quadrifilar hemispherical helix at a normalized circumference of 0.80λ .

II. CONCLUSION

The top-fed bifilar hemispherical helix has been shown to have some useful qualities over approximately a 14% bandwidth, including operation purely in the axialnull mode, a very flat gain curve (less than 0.8 dB variation) and a moderately low VSWR of about 3.5 with a variation of less than 0.5. The antenna produced modest circular polarization over small beam widths and a limited bandwidth on either side of bore sight and elliptical polarization in general. The geometry of the hemisphere allows for a much more stable and compact version of the spherical helix, and thus an attractive alternative from a mechanical perspective. Further investigation of this antenna could prove beneficial. One factor that requires further examination is the radius of conductor, as a thicker conductor would likely improve impedance characteristics and possibly radiation characteristics (such as polarization). It may also prove that slight rotation of one of the arms about the axis could control the depth of the null at bore sight, and may even improve the characteristics of the antenna. The side-fed quadrifilar hemispherical helix has proven to be less promising than the previous design, owing primarily to its very high (oscillatory) VSWR. As a result, the antenna would seem to provide no new improvements over existing designs. It may turn out, however, that by increasing the conductor diameter there could be some improvement in the VSWR; however, it is expected that the oscillatory nature of this parameter over a range of frequencies would remain, thus maintaining the difficulty.. If we increase the width of the gap, the resonant frequency will change more obviously.

REFERENCES

- [1] Kraus, J. D., Helical beam antennas, Electronics, Vol. 20, 109-111, 1947.
- [2] John D. Kraus, Antennas, second edition, TATA McGraw Hill
- [3] Nakano, H., Y. Samasa, and J. Yamauchi, Axial mode helical antennas, IEEE Transactions on Antennas and Propagation, Vol. 34, No. 9, 489-509, 1986.
- [4] Nakano, H., H. Takeda, T. Honma, H. Mimaki, and J. Yamauchi, Extremely low-profile helix radiating a circularly polarized wave, IEEE Transactions on Antennas and Propagation, Vol. 39, No. 6, 754-757, 1991.
- [5] Nakano, H. and H. Mimaki, Radiation from a short helical antenna backed by a cavity, Electronics Letters, Vol. 31, No. 8, 602-604, 1995.
- [6] Hui, H. T., K. Y. Chan, and E. K. N. Yung, The low-profile hemispherical helical antenna with circular polarization radiation over a wide angular range, IEEE Transactions on Antennas and Propagation, Vol. 51, No. 6, 1415-1418, 2003.
- [7] Nakano, H., K. Sato, H. Mimaki, and J. Yamauchi, A long helical antenna wound on a dielectric rod, Proceedings of ISAP, POS-A-27, 965-968, 2004.
- [8] Maja Škiljo and Zoran Blažević, Helical Antennas in Satellite Radio Channel publication at: <https://www.researchgate.net/publication/221913796>, 20004
- [9] M. Hosseini, M. Hakkak, Senior Member, Design of a Dual-Band Quadrifilar Helix Antenna, IEEE antennas and wireless propagation letters, vol. 4, 2005
- [10] Ilcev, S. D., Global Mobile Satellite Communications: For Maritime, Land and Aeronautical Applications, Springer, Berlin, 2005.
- [11] Djordjevic, A. R., A. G. Zajic, M. M. Llic, and G. L. Stuber, Optimization of helical antennas, IEEE Antennas and Propagation Magazine, Vol. 48, 107-115, 2006.
- [12] Wu, Z.-H., W.-Q. Che, B. Fu, P.-Y. Lau, and E. K. N. Yung, Axial mode elliptical helical antenna with parasitic wire for CP bandwidth enhancement, IET Microwave. Antennas Propagation., Vol. 1, No. 4, 943-94, 2007.
- [13] Yang, F., P. Zhang, C.-J. Guo, and J.-D. Xu, Axial mode elliptical helical antenna with variable pitch angle, Electronics Letters, Vol. 44, No. 9, 1103-1104, 2008.
- [14] SSR Rao, T.V.Ramana, E Sarva Rameswarudu, bandwidth and gain enhancement in helical antenna For ku band and satellite communication applications, IJRET: International Journal of Research in Engineering & Technology eISSN: 2319-1163 | pISSN: 2321-7308, 2009.
- [15] Alexandru Takacs, et al., Miniaturization of Quadrifilar Helix Antenna for VHF Band Applications, IEEE Conference, Antennas & Propagation Conference (LAPC) pp. 597-600, 2009.
- [16] Gao S et al., Antennas for modern small satellites, IEEE Antennas Propagation Magazine, Vol. 51, No. 4, pp. 40-56, 2009.
- [17] Nan Gao, Shaobin Liu, Yinsheng Wei, Zhaoyang, Quadrifilar Helix Antenna With Mechanically Tunable Compact Geometry, IEEE, 978-1-4244-5708-3/10/2010
- [18] Wang, J.-L. and C.-S. Liu, Development and application of INMARSAT satellite communication system, Proceedings of International Conference on Instrumentation, Measurement, Computer, Communication and Control, 619-621, Beijing, China, 2011.
- [19] Alexandru Takacs, et al., Miniaturization technique for quadrifilar helix antenna, IEEE Conference, Antennas and Propagation Society International Symposium (APSURSI) pp. 1-2, 2012
- [20] Boccia L, et al., Space Antenna Handbook. Hoboken, NJ, USA: Wiley, 2012.